Ionization dynamics through a Fano resonance: Time-domain interpretation of spectral amplitudes

Antoine Desrier, Alfred Maquet, Richard Taïeb, and Jérémie Caillat*
Sorbonne Université, CNRS, Laboratoire de Chimie Physique-Matière et Rayonnement, LCPMR, F-75005 Paris, France

(Received 21 September 2018; published 7 November 2018)

We investigate a conjecture used in recent experiments to reconstruct the complete dynamics of Fano autoionization processes out of measured spectral amplitudes [Gruson *et al.*, Science **354**, 734 (2016); Beaulieu *et al.*, Science **358**, 1288 (2017); Busto *et al.*, J. Phys. B: At. Mol. Opt. Phys. **51**, 044002 (2018)]. The validity of the conjecture is established analytically within the formalism of Fano, and tested numerically on model atoms displaying adjustable autoionizing states. A general condition for which the conjecture is valid, beyond the Fano case, is then derived.

DOI: 10.1103/PhysRevA.98.053406

I. INTRODUCTION

Amongst the variety of phenomena explored in the time domain by attosecond (1 as $= 10^{-18}$ s) time-resolved spectroscopy [1,2], a very fundamental one is photoemission itself. In the late 2000s, cutting edge experiments performed in atoms [3,4], molecules [5], and solids [6] evidenced for the first time ultrashort "ionization delays." These are equivalent to Wigner-Smith group delays [7,8] applied to photoemission: they reflect how the dynamics of a photoelectron is affected by species- and channel-specific short-range interactions with the composite parent ion, and are encoded in the scattering phase of the associated wave functions. Photoemission group delays are accessed experimentally through interferometric measurements of photoemission amplitudes, and more specifically of their phases [9–12].

The relevance of mere "delays" to accurately characterize the dynamics of photoemission is however restricted to smooth continuua displaying no or little structure, where the scattering phase varies linearly within the bandwidth of the photoelectron wave packets. Reducing photoemission dynamics to a single group delay no longer applies when the wave packet builds up across a significantly structured continuum. This is typically the case for a Fano resonance—a photoemission process taking place competitively through an autoionizing metastable state and directly to the continuum [13].

It is only recently that comprehensive ways of looking at autoionization in the time domain have been proposed [14–21], motivated by the perspectives of probing and controlling these dynamics experimentally with unprecedented, subfemtosecond, resolution [22–27]. Complete Fano resonance buildups were monitored experimentally for the first time using an original interferometric scheme dubbed Rainbow-RABBIT [28] and with attosecond transient absorption spectroscopy [29], both on the He($2s2p$) prototype [13]. An extension of the Rainbow-RABBIT technique was used shortly after to reconstruct the anisotropic, polarization sensitive, photoemission dynamics of chiral molecules in a flat continuum as well as in the vicinity of an autoionizing state [30].

The present work addresses the reconstruction method introduced in [28], based on a time-energy analysis of the scattering amplitudes $A(E)$ measured around a Fano resonance.[1] In spite of being appreciably straightforward, the experimental data treatment relies on a *conjecture* consisting in giving sense to a "time-domain amplitude" defined as

$$a(t) := \int_{-\infty}^{+\infty} A(E) e^{-iEt}\, dE. \tag{1}$$

Switching between the spectral and time domains using Fourier relations is almost a reflex inherited from wave mechanics. In quantum physics, it applies to *wave functions* as prescribed by the time-dependent Schrödinger equation (TDSE). However, when applied to *amplitudes* as in Eq. (1) the validity of time-domain interpretations is not granted by the first principles of quantum mechanics. In this context, the aim of this work is to establish the conditions under which $a(t)$ is a physically meaningful quantity, first in the specific case of Fano autoionization and then in a broader perspective.

The paper is organized as follows. First, we specify in Sec. II the above-mentioned conjecture within the formalism established by Fano. Then, in Sec. III, we demonstrate analytically that the conjecture is indeed valid for any Fano autoionization process. In Sec. IV, we illustrate the analytical result and test the main approximation used in their derivation by means of numerical simulations performed on simple model atoms. Finally, we derive a very general condition under which the conjecture is valid, beyond the Fano case, in Sec. V. The conclusions are given in Sec. VI. Technical details on the analytical derivations and numerical simulations are provided in the Appendixes.

*jeremie.caillat@sorbonne-universite.fr

[1]The possibility to *measure* the phase of a photoemission amplitude using pump-probe interferometry has been thoroughly investigated over the past years [9,10,12,31–33]. It is still the subject of open questions (see, e.g., Refs. [34–36]) that we do not address in the present paper, which instead focuses on the time-domain *interpretation*.

Atomic units are used in Eq. (1) and all through the article unless otherwise stated.

II. FANO SPECTRAL AMPLITUDES AND THEIR CONJECTURED TIME-DOMAIN INTERPRETATIONS

In this section, we first provide a short account of the formalism developed by Fano to model autoionizing resonances in the spectral domain, and then expose the conjectured time-domain interpretation of spectral amplitudes discussed in this paper.

A. Fano's formalism: Autoionization in the spectral domain

The formalism established by Fano [13] to describe autoionization in the spectral domain uses a partitioning of the system's eigenstates ($|\Psi_E\rangle$) at energies $E > 0$ around the resonance in terms of *bound* ($|\phi_b\rangle$) and *scattering* ($|\phi_E\rangle$) contributions,[2]

$$|\Psi_E\rangle = |\phi_b\rangle + |\phi_E\rangle, \tag{2}$$

each of them being assigned appropriate asymptotic behaviors.

The bound part typically corresponds to a doubly excited state (such as the $2s2p$ configuration of He), while the scattering part is a relaxed singly ionized state with an electron in the continuum [$\mathrm{He}(1s) + e^-$]. Any population of $|\phi_b\rangle$ eventually transfers into $|\phi_E\rangle$ due to electron correlation, within a time scale given by the resonance lifetime. It is the coherence of the process which results in interferences between the two paths, and shapes the early times of the correlation driven scattering dynamics of the photoelectron.

The approach further consists in expanding the scattering component $|\phi_E\rangle$ in terms of reference continuum states $|\varphi_E\rangle$ virtually uncoupled from the bound component $|\phi_b\rangle$. For a resonance with characteristic energy E_R and width Γ_R, Fano derived the following expression for the probability amplitude $A(E)$ to end up in state $|\varphi_E\rangle$ upon absorption of a photon with frequency $\omega = E + I_p$ (I_p is the ionization potential):

$$A(E) = \mathcal{F}(\omega) V_E \frac{\varepsilon + q}{\varepsilon + i}. \tag{3}$$

In this compact formula, V_E is the direct transition amplitude from the initial bound state $|\phi_0\rangle$ towards $|\varphi_E\rangle$, $\varepsilon = 2(E - E_R)/\Gamma_R$ is the reduced energy, and the Fano parameter q is proportional to the ratio V_E/V_b, where V_b is the transition amplitude from $|\phi_0\rangle$ towards $|\phi_b\rangle$; see [13] for more details. In order to take into account finite pulse effects, we have included in this expression the driving field amplitude $\mathcal{F}(\omega)$. As evidenced by Eq. (3), the scattering phase $\arg A(E)$ undergoes two π jumps within a spectral range of $\sim\Gamma_R$ around E_R: a sharp one occurs at $\varepsilon = -q$ as the numerator of $A(E)$ vanishes and changes sign and another one, smoothed over the resonance width, is centered on the resonance energy as the real part of the denominator vanishes and changes sign.

[2]To keep the notations simple, we discard the additional parameters that, besides the energy E, allow one to fully specify the considered continuum states and therefore to distinguish the various possible ionization channels.

The essential approximation made by Fano to derive Eq. (3) is to consider the direct transition amplitude towards the scattering continuum, V_E, to be constant within a range of a few Γ_R in the vicinity of the resonance. This is a very reasonable approximation, as highlighted by the remarkably broad efficiency of the Fano profile to model with high accuracy resonances in nuclear, atomic, molecular, and nanophysics, and even classical oscillators; see, for example, the review in [37]. As we will see in Sec. III, it is also the only approximation needed to validate the time-domain interpretation of $A(E)$ made in [21,28,30].

B. Conjecture: Autoionization in the time domain

In the time domain, the most straightforward characteristic of a Fano resonance is its lifetime, which coincides with half the photoemission delay *at resonance* [38,39]. It is, however, only representative of the exponential decay of the autoionizing state into the continuum, discarding the impact of interferences on early time dynamics. More detailed temporal insight on resonances can be obtained by considering the "survival probability" introduced by Krylov and Fock [40]. It notably displays deviations from the exponential law at small and large times [41]. Still, it focuses on the resonance *decay*, considering that only the bound part of the resonance is initially populated. It may be suitable for describing an Auger or a nuclear decay but excludes other processes such as Fano resonances.

In contrast, the approaches based on the Rainbow-RABBIT technique [21,28,30] mentioned in the Introduction provide a whole picture of the Fano resonance as it builds up in time. The conjecture it relies on consists in relating the temporal amplitude $a(t)$, defined in Eq. (1), to two observables: the ionization rate, $I(t)$, according to

$$I(t) = \frac{1}{2\pi}|a(t)|^2, \tag{4}$$

and the photoelectron spectrum as it builds up in time during the process, $\mathcal{P}(E,t)$, according to

$$\mathcal{P}(E,t) = \frac{1}{4\pi^2}\left|\int_{-\infty}^{t} a(t')e^{iEt'}\,dt'\right|^2. \tag{5}$$

The latter is hereafter referred to as the transient photoelectron spectrum (TPES).

The two quantities being related through

$$I(t) = \frac{\partial}{\partial t}\int_{-\infty}^{+\infty} \mathcal{P}(E,t)\,dE, \tag{6}$$

it is easy to show that Eq. (5), when valid, implies Eq. (4) (see Appendix A 1). We will thus focus on Eq. (5). This puts forward the limited inverse Fourier transform (LIFT) of $a(t)$, defined as

$$\mathcal{A}(E,t) := \frac{1}{2\pi}\int_{-\infty}^{t} a(t')e^{iEt'}\,dt', \tag{7}$$

which is the main tool inherited from time-frequency analysis in the present study. The $(2\pi)^{-1}$ normalization factor in Eqs. (4) and (7), and squared in Eq. (5), is here to ensure consistency between the Fourier transform and its inverse, throughout the article.

III. ANALYTICAL VALIDATION OF THE CONJECTURE

In this section, we demonstrate analytically that the conjectured interpretation of $a(t)$ is indeed valid for a Fano resonance. To this end, we compare the dynamics *inferred* from $a(t)$ to the *actual* Fano dynamics as initially derived by Mercouris and co-workers [16,17].

A. Actual buildup of the continuum wave packet

In the framework provided by Fano's approach, the evolution of the *continuum* wave packet $|\psi_{\rm sca}(t)\rangle$ during its formation and propagation is obtained by expanding it on the reference scattering states $|\varphi_E\rangle$,

$$|\psi_{\rm sca}(t)\rangle = \int_{-\infty}^{+\infty} c_E(t)|\varphi_E\rangle e^{-iEt}\,dE. \tag{8}$$

In this notation, one must keep in mind that the actual support of the coefficients $c_E(t) = \langle\varphi_E|\psi_{\rm sca}(t)\rangle$ is restricted, by definition, to $E > 0$. The TPES is directly related to $c_E(t)$ through

$$\mathcal{P}(E,t) = |c_E(t)|^2. \tag{9}$$

Therefore, the conjecture (5) is verified if and only if the modulii of $\mathcal{A}(E,t)$ [defined in Eq. (7)] and of $c_E(t)$ are equal.

A comprehensive derivation of the analytical expression for $c_E(t)$ is detailed in [16,17].[3] It reads

$$c_E(t) = \frac{V_E}{i}\left[\mathcal{G}(E,t)\frac{(q+\varepsilon)}{(\varepsilon+i)} - \mathcal{G}\left(E_{\rm R} - i\frac{\Gamma_{\rm R}}{2}, t\right) \times \frac{(q-i)}{(\varepsilon+i)} e^{i\varepsilon\frac{\Gamma_{\rm R}}{2}t} e^{-\frac{\Gamma_{\rm R}}{2}t}\right], \tag{10}$$

where

$$\mathcal{G}(E,t) := \frac{1}{2\pi}\int_{-\infty}^{t} \mathcal{E}(t')e^{i(E+I_p)t'}\,dt' \tag{11}$$

is the LIFT of the field temporal amplitude

$$\mathcal{E}(t) = \int_{-\infty}^{+\infty} \mathcal{F}(\omega)e^{-i\omega t}\,d\omega. \tag{12}$$

One can easily verify with Eqs. (10) and (3) that the asymptotic value of $c_E(t)$ is proportional to the transition amplitude $A(E)$,

$$\lim_{t\to+\infty} c_E(t) = \frac{1}{i}A(E), \tag{13}$$

a result reminiscent of the perturbative treatment underlying the Fano formalism.

B. Reconstruction of the continuum wave packet

We now derive the analytical expression of $\mathcal{A}(E,t)$ for a Fano resonance, that we will compare to the one of the time-dependent coefficients $c_E(t)$ given in Eq. (10). Assuming that V_E is constant ($= V_{\bar{E}}$) over the bandwidth of $A(E)$, the temporal amplitude [Eq. (3)] for a Fano resonance verifies[4]

$$\frac{1}{V_{\bar{E}}}a(t) = \mathcal{E}(t)e^{I_p t} + (q-i)\frac{\Gamma_{\rm R}}{2} \times \int_{-\infty}^{+\infty} \frac{\mathcal{F}(\omega')}{\omega' - \omega_{\rm R} + i\frac{\Gamma_{\rm R}}{2}} e^{-i(\omega'-I_p)t}\,d\omega'. \tag{14}$$

Therefore, the LIFT of $a(t)$, defined in Eq. (7), reads

$$\begin{aligned}\frac{1}{V_{\bar{E}}}\mathcal{A}(E,t) &= \mathcal{G}(E,t) + (q-i)\frac{\Gamma_{\rm R}}{2}\int_{\omega'=-\infty}^{+\infty} \frac{\mathcal{F}(\omega')}{\omega' - \omega_{\rm R} + i\frac{\Gamma_{\rm R}}{2}} \frac{1}{2\pi}\int_{t'=-\infty}^{t} e^{i(\omega-\omega')t'}\,dt'\,d\omega' \\ &= \mathcal{G}(E,t) - (q-i)\frac{\Gamma_{\rm R}}{2}\frac{i}{2\pi}\int_{-\infty}^{+\infty} \frac{\mathcal{F}(\omega')}{\omega' - \omega_{\rm R} + i\frac{\Gamma_{\rm R}}{2}} \lim_{t_0\to-\infty} \frac{[e^{i(\omega-\omega')t} - e^{i(\omega-\omega')t_0}]}{\omega'-\omega}\,d\omega'.\end{aligned} \tag{15}$$

In order to get a formula involving $\mathcal{G}$ functions in each term, as in Eq. (10), we reintroduce the pulse temporal profile $\mathcal{E}$, where $\mathcal{F}$ appears in the last equation. This gives

$$\begin{aligned}\frac{1}{V_{\bar{E}}}\mathcal{A}(E,t) &= \mathcal{G}(E,t) - (q-i)\frac{\Gamma_{\rm R}}{2}\frac{i}{2\pi}\int_{\omega'=-\infty}^{+\infty} \frac{(2\pi)^{-1}\int_{t'=-\infty}^{+\infty}\mathcal{E}(t')e^{i\omega' t'}\,dt'}{\omega' - \omega_{\rm R} + i\frac{\Gamma_{\rm R}}{2}} \lim_{t_0\to-\infty} \frac{[e^{i(\omega-\omega')t} - e^{i(\omega-\omega')t_0}]}{\omega'-\omega}\,d\omega' \\ &= \mathcal{G}(E,t) - (q-i)\frac{\Gamma_{\rm R}}{2}\frac{i}{(2\pi)^2}\int_{t'=-\infty}^{+\infty}\mathcal{E}(t')\left[e^{i\omega t}J(t'-t) - \lim_{t_0\to-\infty} e^{i\omega t_0}J(t'-t_0)\right]dt',\end{aligned} \tag{16}$$

where we introduced

$$J(\tau) := \int_{-\infty}^{+\infty} \frac{e^{i\omega'\tau}}{\left(\omega' - \omega_{\rm R} + i\frac{\Gamma_{\rm R}}{2}\right)(\omega'-\omega)}\,d\omega'. \tag{17}$$

Contour integrations give (see Appendix A 2)

$$e^{i\omega t}J(t'-t) = -2\pi i\, e^{i\omega t}[1-\Theta(t'-t)]\left[\frac{e^{i(\omega_{\rm R} - i\frac{\Gamma_{\rm R}}{2})(t'-t)}}{\omega - \omega_{\rm R} + i\frac{\Gamma_{\rm R}}{2}} - \frac{e^{i\omega(t'-t)}}{\omega - \omega_{\rm R} + i\frac{\Gamma_{\rm R}}{2}}\right], \tag{18}$$

[3] A similar expression is derived in [18] for a Fano resonance triggered by a *sudden pulse*.

[4] The dynamics of atomic autoionization with a sudden pulse was also investigated theoretically in [14]. In this paper, the conjecture corresponding to Eq. (4) is implicit [see Eq. (2) of that reference]. Their results are compatible with the present expression for $a(t)$ [Eq. (14)] in the limit $\mathcal{E}(t) \to \delta(t)$.

where Θ is the Heaviside function and

$$\lim_{t_0\to-\infty} e^{i\omega t_0} J(t'-t_0) = 0. \tag{19}$$

Inserting this in Eq. (16) leads to

$$\frac{1}{V_{\bar{E}}}\mathcal{A}(E,t) = \mathcal{G}(E,t) - \frac{(q-i)}{(\varepsilon+i)}\frac{1}{2\pi}\left[e^{i(\omega-\omega_R+i\frac{\Gamma_R}{2})t} \underbrace{\int_{t'=-\infty}^{t} \mathcal{E}(t') e^{i(\omega_R - i\frac{\Gamma_R}{2})t'}\, dt'}_{2\pi\mathcal{G}(E_R - i\frac{\Gamma_R}{2},t)} - \underbrace{\int_{t'=-\infty}^{t} \mathcal{E}(t')\, e^{i\omega t'}\, dt'}_{2\pi\mathcal{G}(E,t)} \right] \tag{20}$$

and we ultimately obtain the sought after expression for the LIFT of $a(t)$,

$$\mathcal{A}(E,t) = V_{\bar{E}}\left[\frac{(\varepsilon+q)}{(\varepsilon+i)}\mathcal{G}(E,t) - \frac{(q-i)}{(\varepsilon+i)} \times e^{i\varepsilon\frac{\Gamma_R}{2}t} e^{-\frac{\Gamma_R}{2}t}\mathcal{G}\left(E_R - i\frac{\Gamma_R}{2}, t\right)\right]. \tag{21}$$

By comparing Eq. (21) with Eq. (10), one immediately sees that

$$\mathcal{A}(E,t) = i c_E(t). \tag{22}$$

This result shows that the LIFT-based analysis of $A(E)$ gives access to a most fundamental quantity: the time-dependent spectral coefficients $c_E(t)$ of the continuum wave packet describing the photoelectron. From there, using the definition of $\mathcal{P}(E,t)$ [Eq. (9)], we obtain Eq. (5). The conjecture according to which the complete buildup dynamics of a Fano resonance can be retrieved from its spectral ionization amplitude $A(E)$ is therefore indeed valid.

IV. NUMERICAL TESTS OF THE "CONSTANT V_E" APPROXIMATION

We have performed numerical simulations in order to illustrate the analytical results derived in the previous section, and to assess the validity of the "constant V_E" approximation.

A. Coupled-channel model

We used a one-dimensional coupled-channel model designed to display an autoionizing state with adjustable energy E_R, width Γ_R, and q parameter. It is defined by a field-free Hamiltonian H_0 explicitly partitioned as two 1D Hamiltonians h_1 and h_2 associated with each of the channels coupled by a V_{cpl} term,

$$H_0 = \begin{pmatrix} h_1 & V_{cpl} \\ V_{cpl} & h_2 \end{pmatrix}. \tag{23}$$

Each of the channel-specific Hamiltonians h_k $(k = 1, 2)$ is assigned a standard form

$$h_k = -\frac{1}{2}\frac{\partial^2}{\partial x^2} + V_k(x), \tag{24}$$

where $V_k(x)$ are potentials adapted to reproduce the desired energy spectra. In the present case, $V_1(x)$ is a Gaussian potential whose parameters (depth and width) set the ionization potential I_p of the model atom. The continuum states of h_1 correspond to the reference scattering states $|\varphi_E\rangle$. The potential $V_2(x)$ was adjusted for h_2 to display a ground state at the same energy as h_1 and an excited *bound* state (with odd symmetry) at an energy located close to E_R, above the ionization threshold of h_1. This excited state corresponds to $|\phi_b\rangle$ in Eq. (2). The coupling term $V_{cpl}(x)$ is a hyper-Gaussian function optimized empirically to obtain the desired resonance parameters, q and Γ_R. This model reproduces very well the features of Fano resonances [42], and is simple enough to allow extensive time-dependent and time-independent numerical simulations.

Here we present results obtained with two such "atoms," with relevent properties summarized in Table I. The first one (atom A) has characteristics close to the ones of He and its $2s2p$ resonance [13], which lies few tens of eV above threshold. The second one (atom B) displays an autoionizing state with comparable width and q parameter, but located very close to the threshold. For each atom, we simulated a resonant photoemission process by solving numerically the TDSE in the presence of a light pulse with adapted central frequency ω_{xuv} and full duration τ_{xuv}. The pulses were assigned $\sin^2$ envelopes centered at $t = 0$, with intensities safely in the perturbative regime.

B. Resonance far from threshold

We first detail our procedure and present the results obtained for atom A. The density of states (DOS) above ionization threshold [38] for this atom is displayed in Fig. 1(a) (see Sec. B 1 for numerical details). It follows a typical decaying law $\sim(2E)^{-1/2}$ on top of which a sharp peak indicates the position of the resonance slightly above 35 eV. We estimated the relative variations of V_E in the vicinity of the resonance through

$$\Delta = \frac{|V_{E_R+\Gamma_R/2} - V_{E_R-\Gamma_R/2}|}{V_{E_R}\Gamma_R}. \tag{25}$$

TABLE I. Characteristic features of the model atoms used in the simulations: ionization potential (I_p), resonance energy (E_R), width (Γ_R), lifetime ($\tau_R = \Gamma_R^{-1}$), and Fano parameter (q). The energy scale refers to the ionization threshold for each atom.

Atom	I_p (eV)	E_R (eV)	Γ_R (meV)	τ_R (fs)	q
A	24.59	35.62	39.2	16.67	−2.98
B	15.53	1.54	57.7	11.32	−2.66

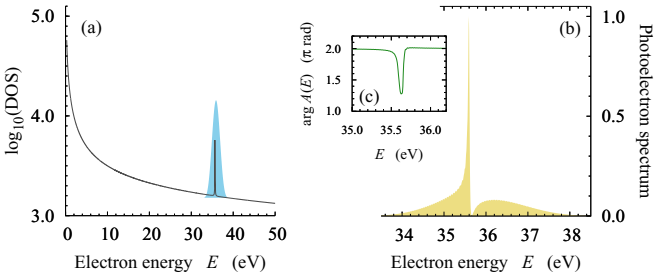

FIG. 1. (a) DOS above ionization threshold (arb. units) for the atom A (gray full curve) and spectral profile of the pulse used in the simulations (blue filled curve); (b) PES $P(E)$ normalized to 1 at its maximum (yellow filled curve); (c) phase arg $A(E)$ in the vicinity of the resonance (green full curve). The pulse parameters are $\omega_{\rm xuv} = 60.33$ eV and $\tau_{\rm xuv} = 2.67$ fs.

For the atom A, it amounts to 4.3×10^{-2} eV^{-1}. We also displayed in Fig. 1(a) the profile of the pulse used in the simulation (blue filled curve). Its central frequency $\omega_{\rm xuv}$ was set to 60.33 eV to reach the vicinity of the resonance, and its duration $\tau_{\rm xuv}$ to 2.67 fs (39 optical cycles), which is significantly smaller than the resonance lifetime $\tau_{\rm R} = 16.67$ fs. Figure 1(b) shows the photoelectron spectrum (PES) $P(E)$, computed from the propagated wave function $\psi(x, t_{\rm end})$ at the end of the simulation ($t_{\rm end} \simeq 130$ fs) using the window method [43] detailed in Appendix B 2. Its asymmetric shape is consistent with the resonance parameters, notably the maximum near $E_{\rm R}$ ($\varepsilon = 0$) and the minimum located at $E = E_{\rm R} - q\Gamma_{\rm R}/2$ ($\varepsilon = -q$), as well as with the pulse parameters (spectral width $\sim$4 eV).

The TPES $\mathcal{P}(E, t)$ were computed using the same technique applied to the propagated wave function $\psi(x, t)$ at various times during the process. The TPES at four illustrative times are displayed in Fig. 2 (yellow filled curves). These numerically exact spectra are representative of the *actual* ionization dynamics. Their evolution is consistent with the chronology of a Fano process [15] and notably with the analytical formula for the coefficients $c_E(t)$ [Eq. (10)], as was already investigated in [16,18]. At the earliest displayed time, in frame (a), the spectrum follows a smooth bell curve reminiscent of the ionizing pulse profile: at such an early time (1.75 fs $\sim$ 10% $\tau_{\rm R}$), the ionization process occurs dominantly through the *direct* path. In frame (b), first signatures of the autoionizing path are already visible. The main peak begins to shrink around the resonance energy, on each side of which satellite structures appear. In frame (c), as the central peak continues to refine and to asymmetrize, it becomes clearer that these satellite structures are oscillations, which result from interferences between the direct and autoionizing paths. Indeed, it is easy to see from the analytical expression of the coefficients $c_E(t)$ in the case of a sudden pulse [see, e.g., Eq. (23) of [18]] that the TPES contain an interference term proportional to $\sin[(E - E_{\rm R})t + \arctan q]$—the spectral frequency (phase) of which increases (decreases) linearly with time—damped by an $\exp(-\Gamma_{\rm R}t/2)$ factor. At the last displayed time in frame (d), the oscillations tighten and the spectrum converges to its final shape [see Fig. 1(b)].

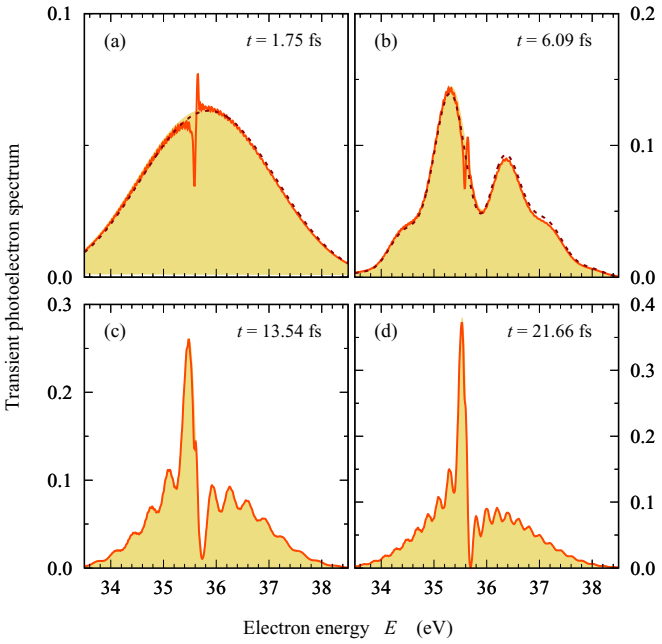

FIG. 2. Transient photoelectron spectra for atom A (pulse parameters specified in the caption of Fig. 1). (a)–(c) Actual TPES, $\mathcal{P}(E, t)$ (yellow filled curves), and reconstructed TPES, $|\mathcal{A}(E, t)|^2$ (orange full curves), at four different times t. The time origin $t = 0$ corresponds to the maximum of the pulse envelope. In frames (a) and (b) the TPES reconstructed out of the analytical amplitudes $A(E)$ is also shown (brown dashed curves). The TPES are normalized consistently with the PES displayed in Fig. 1(b).

Besides, still for atom A, we extracted the spectral amplitude $A(E)$ out of the final wave function $\psi(x, t_{\rm end})$. The modulus is simply given as $|A(E)| = \sqrt{P(E)}$, while the phase arg $A(E)$ was computed using an adapted numerical interferometric scheme detailed in Appendix B 3. The spectral variations of $A(E)$, displayed in Fig. 1(c), are typical of a Fano resonance with the two consecutive $\sim\pi$ jumps already discussed in Sec. II A. From $A(E)$, we computed the temporal amplitude $a(t)$ [Eq. (1)] and its LIFT $\mathcal{A}(E, t)$ [Eq. (7)]. The reconstructed TPES, $|\mathcal{A}(E, t)|^2$, are shown in Fig. 2 (orange full curves), at the same times as $\mathcal{P}(E, t)$ for comparison. Apart from a spurious narrow structure around $E_{\rm R}$ visible at the earlier times [frames (a) and (b), hardly in frame (c)], the agreement between the *actual* and the *reconstructed* spectra is excellent. We identified the spurious structure as a numerical artifact due to an imperfect convergence of the "final" wave function $\psi(x, t_{\rm end})$ used to compute $A(E)$. To verify this, we also computed the reconstructed TPES using the *analytical* expression for $A(E)$ [Eq. (3)], with the Fano and pulse parameters adapted to our simulations, and displayed them in frames (a) and (b) of Fig. 2 (brown dashed curves). The spurious structure is indeed absent from these analytical reconstructed TPES, which almost perfectly reproduce the actual TPES (yellow filled curves). In conclusion, the results obtained with atom A illustrate and confirm the validity of Eq. (5) when V_E is nearly constant.

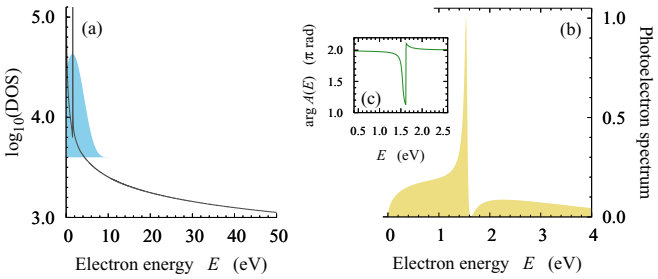

FIG. 3. (a) DOS above ionization threshold (arb. units) for the atom B (gray full curve) and spectral profile of the pulse used in the simulations (blue filled curve); (b) PES $P(E)$ normalized to 1 at its maximum (yellow filled curve); (c) phase arg $A(E)$ in the vicinity of the resonance (green full curve). The pulse parameters are $\omega_{\rm xuv} = 17.06$ eV and $\tau_{\rm xuv} = 0.97$ fs.

C. Resonance near threshold

We repeated the procedure for atom B, which possesses a resonance much closer to the ionization threshold and for which considering V_E as constant is questionable. Here $\Delta = 2.1\times10^{-1}$ eV^{-1} [Eq. (25)], i.e., one order of magnitude larger than for atom A. The DOS above threshold is shown in Fig. 3(a) together with the ionizing pulse profile ($\omega_{\rm xuv} = 17.06$ eV and $\tau_{\rm xuv} = 0.97$ fs, i.e., four cycles). We used a broader pulse than for atom A on purpose, in order to make it significantly overlap the ionization threshold. This strongly affects the final PES (computed here at $t_{\rm end} \simeq 250$ fs), which abruptly vanishes at $E = 0$; see Fig. 3(b). The phase arg $A(E)$ displayed in Fig. 3(c) is consistent with the resonance parameters.

The *actual* transient spectra $\mathcal{P}(E,t)$ are displayed in Fig. 4 (yellow filled curves) at four times close to the ones chosen for atom A. Their evolution is similar to the one in atom A, notably the time-dependent spectral frequency of the transient oscillations, which does not depend on the resonance parameters. The two main differences with respect to atom A are (i) the main peak building up over a somehow different time scale because of the different lifetime and (ii) a more pronounced asymmetry even at the earliest times [frame (a)] due to the nonconstant V_E and to the above-mentioned cutoff at $E = 0$.

The *reconstructed* ones, $|\mathcal{A}(E,t)|^2$, are overlaid on the same figure (orange full curves). As with atom A, they present a spurious narrow structure near $E_{\rm R}$ at early times [frames (a) and (b)] resulting from an imperfectly converged $\psi(x, t_{\rm end})$ used to compute them. Apart from this numerical artifact, it is clear that the agreement between $|\mathcal{A}(E,t)|^2$ and $\mathcal{P}(E,t)$ at the earliest displayed time [frame (a)] is not as good as for atom A. This is a direct manifestation of non-negligible variations of V_E within the wave-packet support, which reshape its "direct continuum" components. Besides, the Fourier analysis does not perfectly reproduce the sharp cutoff at $E = 0$. Thus the reconstructed TPES in frames (a) and (b) slightly extend below the ionization threshold. It is nevertheless noteworthy that a qualitative agreement between the shape and magnitude of $\mathcal{P}(E,t)$ and $|\mathcal{A}(E,t)|^2$ remains in spite of particularly unfavorable conditions. Moreover, the excellent quantitative agreement between the reconstructed and actual TPES is recovered quickly, as can be seen already in frame (b) and

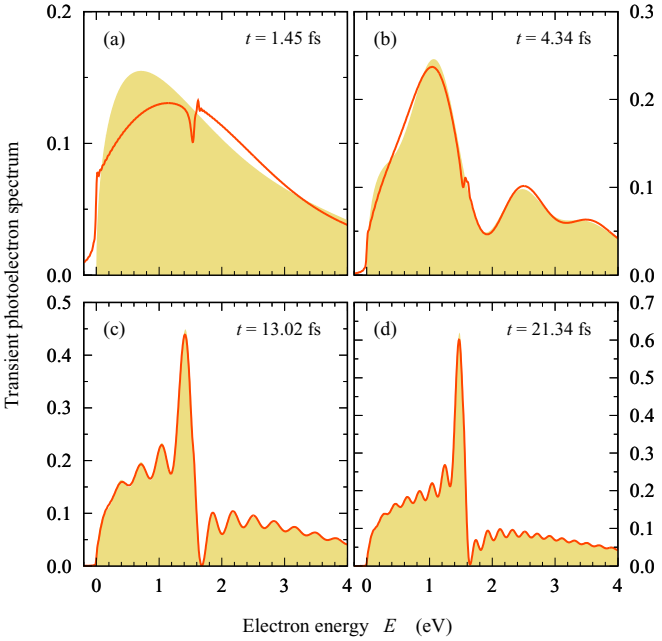

FIG. 4. Transient photoelectron spectra for atom B (pulse parameters specified in the caption of Fig. 3). (a)–(c) Actual TPES, $\mathcal{P}(E,t)$ (yellow filled curves), and reconstructed TPES, $|\mathcal{A}(E,t)|^2$ (orange full curves), at four different times t. The time origin $t = 0$ corresponds to the maximum of the pulse envelope. The TPES are normalized consistently with the PES displayed in Fig. 3(b).

confirmed in frames (c) and (d). Therefore, the results obtained with atom B seem to indicate that the "constant V_E" approximation, needed to validate the conjectured Eq. (5), is robust even for Fano resonances near threshold.

V. TIME-DOMAIN INTERPRETATION OF SPECTRAL AMPLITUDES: GENERAL DOMAIN OF VALIDITY

The analytical and numerical results presented and discussed above suggest to seek further for *general* conditions under which the temporal amplitude $a(t)$ and its LIFT are physically relevent quantities. To address this, we now step away from the Fano paradigm and simply consider a wave packet expressed as in Eq. (8), where each $|\varphi_E\rangle$ is the projection of an eigenstate of energy E on a given reference partition or set. We also assume that the time-dependent coefficients of this wave packet, $c_E(t)$, and A_E are related through Eq. (13). The spectral amplitude $A(E)$ is in turn used to define the temporal amplitude $a(t)$ according to Eq. (1). The wave packet has a finite norm; therefore, $A(E)$ and its Fourier transform $a(t)$ are square integrable functions. From there, we want to establish the condition(s) under which the LIFT of $a(t)$, $\mathcal{A}(E,t)$, and the time-dependent coefficients, $c_E(t)$, verify Eq. (22).

First, taking the time derivative of Eq. (22) with the definition of $\mathcal{A}(E,t)$ [Eq. (7)] gives

$$a(t)e^{iEt} = i\dot{c}_E(t), \tag{26}$$

where we used the notation $\dot{c}_E(t) = \partial c_E(t)/\partial t$. A *necessary* condition for Eq. (26) [and therefore Eq. (22)] to be fulfilled is

that $\dot{c}_E(t)e^{-iEt}$ is independent of E, since $a(t)$ is by definition independent of E.

We can moreover show that it is a *sufficient* condition, using the connections of $A(E)$ with $a(t)$ on the one hand, and with $c_E(t)$ on the other hand. Indeed, Eq. (1) implies

$$A(E) = \frac{1}{2\pi}\int_{-\infty}^{+\infty} a(t)e^{iEt}\,dt \tag{27}$$

and Eq. (13) implies

$$A(E) = \frac{i}{2\pi}\lim_{\tau\to+\infty}\int_{-\infty}^{\tau} \dot{c}_E(t)\,dt \tag{28}$$

$$= \frac{1}{2\pi}\int_{-\infty}^{+\infty} [i\dot{c}_E(t)e^{-iEt}]e^{iEt}\,dt. \tag{29}$$

With that last expression, we see that if $i\dot{c}_E(t)e^{-iEt}$ does not depend on E, then it is the Fourier transform of $A(E)$—just as $a(t)$ is according to Eq. (27). Unicity of the Fourier transform then implies Eq. (26).

Hence Eq. (22) is exactly fulfilled if and only if

$$\frac{\partial}{\partial E}\left[\frac{\partial c_E(t)}{\partial t}e^{-iEt}\right] = 0. \tag{30}$$

A physical interpretation of that condition is that the spectral components of the wave packet are homogeneously "fed" over time. Any structuring of the resulting wave packet is the consequence of interferences occurring during the buildup process. It is noteworthy that we made here very little assumptions on the nature of the wave packet,[5] on the nature of the process populating the continuum states $|\varphi_E\rangle$, nor on the way the spectral amplitude is potentially measured experimentally. This is therefore a very general result.

VI. CONCLUSIONS

In this article, we have established that the complete dynamics of a Fano autoionization process could be retrieved out of the Fourier transform $a(t)$ of the associated transition amplitude $A(E)$—a quantity that can be accessed experimentally under conditions discussed elsewhere (see [28] and references therein). The demonstration relies on a single approximation (a direct transition amplitude towards the continuum, V_E, which is spectrally constant), which is inherent to the Fano formalism and the validity of which is warranted by the broad applicability of the latter. It turns out that the limited inverse Fourier transform of $a(t)$, $\mathcal{A}(E,t)$, exactly coincides, up to a i factor, to the time-dependent coefficient $c_E(t)$ of the quantum wave packet describing the photoelectron. The analytical demonstration was illustrated with simulations performed on simple model atoms displaying autoionizing states, the results of which highlight the robustness of the "constant V_E" approximation.

Eventually, we have identified a general condition under which $\mathcal{A}(E,t)$ is equal to $ic_E(t)$ beyond the particular case of Fano resonances. This provides a unified framework within which the dynamics of a quantum wave packet can be retrieved out of its spectral scattering amplitudes $A(E)$ through simple Fourier analysis. Our reasoning makes little assumption on the nature of the wave packet and none on the way the spectral amplitudes are measured. It may therefore have broad implications ranging further than the particular case of a Fano resonance monitored in time by photoelectron interferometry [21,28,30]—in a context where theoretical inputs are required not only to support experimental measurements, but most importantly for processing the measured data towards meaningful time-domain interpretations.

[5]It is nonetheless easy to verify that the coefficients $c_E(t)$ for a Fano resonance [Eq. (10)] fulfill condition (30).

ACKNOWLEDGMENT

This project is supported by French state funds managed by the ANR programme No. ANR-15-CE30-0001-01-CIMBAAD and the LABEX No. Plas@Par-ANR-11-IDEX-0004-02.

APPENDIX A: ANALYTICS

1. How Eq. (5) implies Eq. (4)

According to the conjectured Eq. (5), the spectrally integrated ionization probability at a given time t reads

$$\int_{-\infty}^{+\infty}\mathcal{P}(E,t)\,dE = \frac{1}{(2\pi)^2}\int_{-\infty}^{+\infty}\left|\int_{-\infty}^{t} a(t')e^{iEt'}\,dt'\right|^2 dE \tag{A1}$$

$$= \frac{1}{(2\pi)^2}\int_{-\infty}^{t}\int_{-\infty}^{t}[a(t')]^{\star}a(t'') \times \underbrace{\int_{-\infty}^{+\infty}[e^{iE(t''-t')}]\,dE}_{2\pi\delta(t''-t')}\,dt''\,dt' \tag{A2}$$

$$= \frac{1}{2\pi}\int_{-\infty}^{t}|a(t')|^2\,dt'. \tag{A3}$$

Therefore,

$$\frac{\partial}{\partial t}\int_{-\infty}^{+\infty}\mathcal{P}(E,t)\,dE = \frac{1}{2\pi}|a(t)|^2. \tag{A4}$$

Since the left-hand side of this last equation corresponds to the ionization rate $I(t)$, we do obtain Eq. (4) as a consequence of Eq. (5).

2. Computation of the integral $J(\tau)$

Equation (16) involves the integral

$$J(\tau) = \int_{\omega'=-\infty}^{\infty} K(\omega',\tau)\,d\omega', \tag{A5}$$

with

$$K(\omega',\tau) = \frac{e^{i\omega'\tau}}{\left(\omega'-\omega_{\mathrm{R}}+i\frac{\Gamma_{\mathrm{R}}}{2}\right)(\omega'-\omega)}. \tag{A6}$$

It displays two poles at ω and $\omega_R - i\frac{\Gamma_R}{2}$ respectively associated with the residues

$$\mathcal{R}(\tau) = \frac{e^{i\omega\tau}}{\omega - \omega_R + i\frac{\Gamma_R}{2}}, \tag{A7}$$

$$\mathcal{R}_R(\tau) = \frac{e^{i(\omega_R - i\frac{\Gamma_R}{2})\tau}}{\omega_R - i\frac{\Gamma_R}{2} - \omega}. \tag{A8}$$

It can be evaluated in the complex plane as

$$J(\tau) = \int_{\mathcal{C}} K(\omega', \tau)\, d\omega' - \int_{\gamma} K(\omega', \tau)\, d\omega', \tag{A9}$$

where $\mathcal{C}$ is a contour consisting of the real axis indented clockwise around the pole at ω, and closed by an arc γ at infinity, either in the upper ($\uparrow$) or lower ($\downarrow$) half plane. The contours are such that the arc in the upper (lower) half plane is followed counterclockwise (clockwise). Choosing the most appropriate contour for the evaluation of $J(\tau)$ depends on the sign of τ.

The full contour integrals are given by the residue theorem:

$$\int_{\mathcal{C}_\uparrow} K(\omega', \tau)\, d\omega' = 0 \tag{A10}$$

because there is no pole in the upper half plane, and

$$\int_{\mathcal{C}_\downarrow} K(\omega', \tau)\, d\omega' = -2i\pi[\mathcal{R}(\tau) + \mathcal{R}_R(\tau)], \tag{A11}$$

since the $\mathcal{C}_\downarrow$ contour encompasses the two poles, which are circled clockwise. The integrals along the arcs depend on the sign of τ as follows.

(i) When $\tau > 0$, the integral along the arc $\gamma_\uparrow$ vanishes. Relations (A9) and (A10) immediately give

$$J(\tau) = 0. \tag{A12}$$

(ii) When $\tau = 0$, the integrals along both $\gamma_\uparrow$ and $\gamma_\downarrow$ vanish. Both contours can thus be used to show that

$$J(0) = 0. \tag{A13}$$

(iii) When $\tau < 0$, the integral along the arc $\gamma_\downarrow$ vanishes and we obtain

$$J(\tau) = -2i\pi\left[\frac{e^{i(\omega_R - i\frac{\Gamma_R}{2})\tau}}{\omega - \omega_R - i\frac{\Gamma_R}{2}} - \frac{e^{i\omega\tau}}{\omega - \omega_R + i\frac{\Gamma_R}{2}}\right]. \tag{A14}$$

APPENDIX B: NUMERICS

1. Evaluation of the densities of states

In the numerical simulations, the positive-energy continuum is replaced by a dense discrete spectrum, with a very narrow spacing ΔE between adjacent levels—such that it can be considered as continuous in practice. The DOS [38] was computed at each discretized $E_k > 0$ of interest as

$$\rho(E_k) = \frac{2}{E_{k+1} - E_{k-1}}, \tag{B1}$$

where E_{k+1} and E_{k-1} are the neighboring eigenenergies. The analysis was restricted to the subspace reached by one-photon absorption, consisting of the states with odd parity. The norm of the DOS computed as such depends on the simulation parameters (box size and grid spacing), without consequence for the present purpose.

2. Evaluation of the photoelectron spectra

We computed numerically the TPES with the window technique [43] adapted to the present two-channel model. The spectrum at a given time t is computed as

$$\mathcal{P}(E, t) = \int_{-\infty}^{+\infty} |\chi_E(x, t)|^2\, dx, \tag{B2}$$

where

$$\chi_E(x, t) = W_E \psi(x, t) \tag{B3}$$

is the propagated wave function filtered with a narrow spectral window operator

$$W_E = \frac{\gamma^2}{(h_1 - E)^2 + i\gamma^2}. \tag{B4}$$

The width of the window, γ, sets the numerical resolution of the spectra. Note that the expression of W_E [Eq. (B4)] involves the field free Hamiltonian h_1, the positive-energy spectrum of which consists in the uncoupled continuum states $|\varphi_E\rangle$ [see the partitioned Hamiltonian H_0 given in Eq. (23)]. At a sufficiently large time t_{end}, the TPES converges numerically to the PES:

$$P(E) = \mathcal{P}(E, t_{\text{end}}). \tag{B5}$$

3. Evaluation of the Fano phase

We retrieved the phase $\arg A(E)$ [displayed in Fig. 1(c) and Fig. 3(c) for atoms A and B, respectively] out of the final wave function $\psi(x, t_{\text{end}})$, using an interferometric scheme based on the same numerical tool as in Appendix B 2. Consistent with the formalism of Fano and with the definition of $A(E)$, the latter scheme takes for reference the wave function $\psi^{(\text{ref})}(x, t_{\text{end}})$ propagated under the same conditions as $\psi(x, t_{\text{end}})$, but *without* the coupling term in the Hamiltonian H_0 [$V_{\text{cpl}} = 0$ in Eq. (23)]. It describes the direct ionization path *only*. The spectral phase we are interested in is therefore the phase difference between the filtered wave functions $\chi_E(x) = W_E\psi(x, t_{\text{end}})$ and $\chi_E^{(\text{ref})}(x) = W_E\psi^{(\text{ref})}(x, t_{\text{end}})$, where W_E is the spectral filter defined in Eq. (B4). We thus coherently added them as

$$\xi_E(x; \theta) = \chi_E(x) + \chi_E^{(\text{ref})}(x)e^{i\theta}, \tag{B6}$$

where θ is an arbitrary phase set manually, and fitted the signal $|\xi_E(x; \theta)|^2$ obtained for various values of θ with the generic function

$$g(\theta) = A + B\, \cos(\theta + \eta). \tag{B7}$$

For sufficiently large distances, the fitting parameter η becomes independent of x and converges to $\arg A(E)$.

[1] S. R. Leone, C. W. McCurdy, J. Burgdörfer, L. S. Cederbaum, Z. Chang, N. Dudovich, J. Feist, C. H. Greene, M. Ivanov, R. Kienberger, U. Keller, M. F. Kling, Z.-H. Loh, T. Pfeifer, A. N. Pfeiffer, R. Santra, K. Schafer, A. Stolow, U. Thumm, and M. J. J. Vrakking, What will it take to observe processes in 'real time'?, Nat. Photon. **8**, 162 (2014).

[2] F. Calegari, G. Sansone, S. Stagira, C. Vozzi, and M. Nisoli, Advances in attosecond science, J. Phys. B: At. Mol. Opt. Phys. **49**, 062001 (2016).

[3] M. Schultze, M. Fieß, N. Karpowicz, J. Gagnon, M. Korbman, M. Hofstetter, S. Neppl, A. L. Cavalieri, Y. Komninos, T. Mercouris, C. A. Nicolaides, R. Pazourek, S. Nagele, J. Feist, J. Burgdörfer, A. M. Azzeer, R. Ernstorfer, R. Kienberger, U. Kleineberg, E. Goulielmakis, F. Krausz, and V. S. Yakovlev, Delay in photoemission, Science **328**, 1658 (2010).

[4] K. Klünder, J. M. Dahlström, M. Gisselbrecht, T. Fordell, M. Swoboda, D. Guénot, P. Johnsson, J. Caillat, J. Mauritsson, A. Maquet, R. Taïeb, and A. L'Huillier, Probing Single-Photon Ionization on the Attosecond Time Scale, Phys. Rev. Lett. **106**, 143002 (2011).

[5] S. Haessler, B. Fabre, J. Higuet, J. Caillat, T. Ruchon, P. Breger, B. Carré, E. Constant, A. Maquet, E. Mével, P. Salières, R. Taïeb, and Y. Mairesse, Phase-resolved attosecond near-threshold photoionization of molecular nitrogen, Phys. Rev. A **80**, 011404 (2009).

[6] A. L. Cavalieri, N. Muller, T. Uphues, V. S. Yakovlev, A. Baltuška, B. Horvath, B. Schmidt, L. Blumel, R. Holzwarth, S. Hendel, M. Drescher, U. Kleineberg, P. M. Echenique, R. Kienberger, F. Krausz, and U. Heinzmann, Attosecond spectroscopy in condensed matter, Nature (London) **449**, 1029 (2007).

[7] E. P. Wigner, Lower limit for the energy derivative of the scattering phase shift, Phys. Rev. **98**, 145 (1955).

[8] F. T. Smith, Lifetime matrix in collision theory, Phys. Rev. **118**, 349 (1960).

[9] V. S. Yakovlev, J. Gagnon, N. Karpowicz, and F. Krausz, Attosecond Streaking Enables the Measurement of Quantum Phase, Phys. Rev. Lett. **105**, 073001 (2010).

[10] J. M. Dahlström, A. L'Huillier, and A. Maquet, Introduction to attosecond delays in photoionization, J. Phys. B: At. Mol. Opt. Phys. **45**, 183001 (2012).

[11] R. Pazourek, S. Nagele, and J. Burgdörfer, Attosecond chronoscopy of photoemission, Rev. Mod. Phys. **87**, 765 (2015).

[12] L. Cattaneo, J. Vos, M. Lucchini, L. Gallmann, C. Cirelli, and U. Keller, Comparison of attosecond streaking and RABBITT, Opt. Express **24**, 29060 (2016).

[13] U. Fano, Effects of configuration interaction on intensities and phase shifts, Phys. Rev. **124**, 1866 (1961).

[14] Z. X. Zhao and C. D. Lin, Theory of laser-assisted autoionization by attosecond light pulses, Phys. Rev. A **71**, 060702 (2005).

[15] M. Wickenhauser, J. Burgdörfer, F. Krausz, and M. Drescher, Time Resolved Fano Resonances, Phys. Rev. Lett. **94**, 023002 (2005).

[16] T. Mercouris, Y. Komninos, and C. A. Nicolaides, Time-dependent formation of the profile of the He $2s2p^1P^o$ state excited by a short laser pulse, Phys. Rev. A **75**, 013407 (2007).

[17] Th. Mercouris, Y. Komninos, and C. A. Nicolaides, Erratum: Time-dependent formation of the profile of the He $2s2p^1P^o$ state excited by a short laser pulse [Phys. Rev. A **75**, 013407 (2007)], Phys. Rev. A **87**, 069905(E) (2013).

[18] W.-C. Chu and C. D. Lin, Theory of ultrafast autoionization dynamics of Fano resonances, Phys. Rev. A **82**, 053415 (2010).

[19] C. M. Granados-Castro and J. L. Sanz-Vicario, Time-resolved resonant photoionization of He using a time-dependent Feshbach method with ultrashort laser pulses, J. Phys. B: At. Mol. Opt. Phys. **46**, 055601 (2013).

[20] P.-Y. Yang and W.-M. Zhang, Buildup of Fano resonances in the time domain in a double quantum dot Aharonov-Bohm interferometer, Phys. Rev. B **97**, 054301 (2018).

[21] D. Busto, L. Barreau, M. Isinger, M. Turconi, C. Alexandridi, A. Harth, S. Zhong, R. J. Squibb, D. Kroon, S. Plogmaker, M. Miranda, Á. Jiménez Galán, L. Argenti, C. L. Arnold, R. Feifel, F. Martín, M. Gisselbrecht, A. L'Huillier, and P. Salières, Time-frequency representation of autoionization dynamics in helium, J. Phys. B: At. Mol. Opt. Phys. **51**, 044002 (2018).

[22] S. Gilbertson, M. Chini, X. Feng, S. Khan, Y. Wu, and Z. Chang, Monitoring and Controlling the Electron Dynamics in Helium with Isolated Attosecond Pulses, Phys. Rev. Lett. **105**, 263003 (2010).

[23] C. Ott, A. Kaldun, P. Raith, K. Meyer, M. Laux, J. Evers, C. H. Keitel, C. H. Greene, and T. Pfeifer, Lorentz meets Fano in spectral line shapes: A universal phase and its laser control, Science **340**, 716 (2013).

[24] C. D. Lin and W.-C. Chu, Controlling atomic line shapes, Science **340**, 694 (2013).

[25] A. Zielinski, V. P. Majety, S. Nagele, R. Pazourek, J. Burgdörfer, and A. Scrinzi, Anomalous Fano Profiles in External Fields, Phys. Rev. Lett. **115**, 243001 (2015).

[26] M. Kotur, D. Guénot, Á. Jiménez-Galán, D. Kroon, E. W. Larsen, M. Louisy, S. Bengtsson, M. Miranda, J. Mauritsson, C. L. Arnold, S. E. Canton, M. Gisselbrecht, T. Carette, J. M. Dahlström, E. Lindroth, A. Maquet, L. Argenti, F. Martín, and A. L'Huillier, Spectral phase measurement of a Fano resonance using tunable attosecond pulses, Nat. Commun. **7**, 10566 (2016).

[27] R. Y. Bello, S. E. Canton, D. Jelovina, J. D. Bozek, B. Rude, O. Smirnova, M. Y. Ivanov, A. Palacios, and F. Martín, Reconstruction of the time-dependent electronic wave packet arising from molecular autoionization, Sci. Adv. **4**, eaat3962 (2018).

[28] V. Gruson, L. Barreau, Á. Jiménez-Galan, F. Risoud, J. Caillat, A. Maquet, B. Carré, F. Lepetit, J.-F. Hergott, T. Ruchon, L. Argenti, R. Taïeb, F. Martín, and P. Salières, Attosecond dynamics through a Fano resonance: Monitoring the birth of a photoelectron, Science **354**, 734 (2016).

[29] A. Kaldun, A. Blättermann, V. Stooß, S. Donsa, H. Wei, R. Pazourek, S. Nagele, C. Ott, C. D. Lin, J. Burgdörfer, and T. Pfeifer, Observing the ultrafast buildup of a Fano resonance in the time domain, Science **354**, 738 (2016).

[30] S. Beaulieu, A. Comby, A. Clergerie, J. Caillat, D. Descamps, N. Dudovich, B. Fabre, R. Géneaux, F. Légaré, S. Petit, B. Pons, G. Porat, T. Ruchon, R. Taïeb, V. Blanchet, and Y. Mairesse, Attosecond-resolved photoionization of chiral molecules, Science **358**, 1288 (2017).

[31] C.-H. Zhang and U. Thumm, Streaking and Wigner time delays in photoemission from atoms and surfaces, Phys. Rev. A **84**, 033401 (2011).

[32] Á. Jiménez-Galán, L. Argenti, and F. Martín, Modulation of Attosecond Beating in Resonant Two-Photon Ionization, Phys. Rev. Lett. **113**, 263001 (2014).

[33] Á. Jiménez-Galán, F. Martín, and L. Argenti, Two-photon finite-pulse model for resonant transitions in attosecond experiments, Phys. Rev. A **93**, 023429 (2016).

[34] S. Heuser, Á. Jiménez Galán, C. Cirelli, C. Marante, M. Sabbar, R. Boge, M. Lucchini, L. Gallmann, I. Ivanov, A. S. Kheifets, J. M. Dahlström, E. Lindroth, L. Argenti, F. Martín, and U. Keller, Angular dependence of photoemission time delay in helium, Phys. Rev. A **94**, 063409 (2016).

[35] E. Lindroth and J. M. Dahlström, Attosecond delays in laser-assisted photodetachment from closed-shell negative ions, Phys. Rev. A **96**, 013420 (2017).

[36] M. Vacher, R. Gaillac, A. Maquet, R. Taïeb, and J. Caillat, Transition dynamics in two-photon ionisation, J. Opt. **19**, 114011 (2017).

[37] A. E. Miroshnichenko, S. Flach, and Y. S. Kivshar, Fano resonances in nanoscale structures, Rev. Mod. Phys. **82**, 2257 (2010).

[38] C. J. Joachain, *Quantum Collisions Theory* (North-Holland Publishing Company, Amsterdam, 1975).

[39] P. C. Deshmukh, A. Kumar, H. R. Varma, S. Banerjee, S. T. Manson, V. K. Dolmatov, and A. S. Kheifets, Wigner-Eisenbud-Smith photoionization time delay due to autoioinization resonances, J. Phys. B: At. Mol. Opt. Phys. **51**, 065008 (2018).

[40] N. Krylov and V. A. Fock, On the 2 conceptions of the uncertainty relation for energy and time, Zh. Eksp. Teor. Fiz. **17**, 93 (1947).

[41] L. Fonda, G. C. Ghirardi, and A. Rimini, Decay theory of unstable quantum systems, Rep. Prog. Phys. **41**, 587 (1978).

[42] B. Yan and C. H. Greene, Coupled-square-well model and Fano-phase correspondence, Phys. Rev. A **95**, 032706 (2017).

[43] K. C. Kulander, K. J. Schaffer, and J. L. Krause, Time-dependent studies of multiphoton processes, in *Atoms in Intense Laser Fields*, edited by M. Gavrila (Academic Press, New York, 1992), p. 247.